

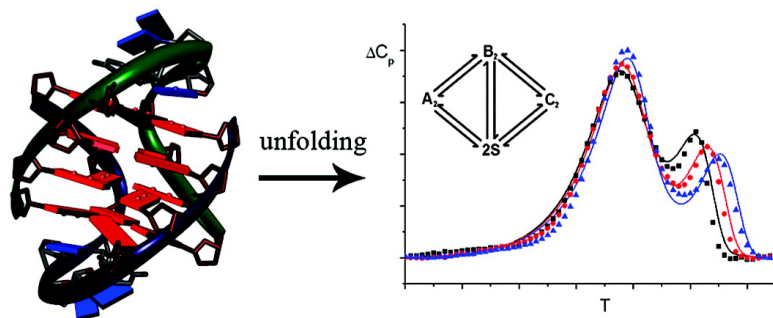
Article

Diverse Polymorphism of G-Quadruplexes as a Kinetic Phenomenon

Iztok Prislan, Jurij Lah, and Gorazd Vesnauer

J. Am. Chem. Soc., **2008**, 130 (43), 14161-14169 • DOI: 10.1021/ja8026604 • Publication Date (Web): 01 October 2008

Downloaded from <http://pubs.acs.org> on February 8, 2009



More About This Article

Additional resources and features associated with this article are available within the HTML version:

- Supporting Information
- Access to high resolution figures
- Links to articles and content related to this article
- Copyright permission to reproduce figures and/or text from this article

[View the Full Text HTML](#)



ACS Publications

High quality. High impact.

Journal of the American Chemical Society is published by the American Chemical Society. 1155 Sixteenth Street N.W., Washington, DC 20036

Diverse Polymorphism of G-Quadruplexes as a Kinetic Phenomenon

Iztok Prislan, Jurij Lah,* and Gorazd Vesnauer*

*University of Ljubljana, Faculty of Chemistry and Chemical Technology, Aškerčeva 5,
1000 Ljubljana, Slovenia*

Received April 11, 2008; E-mail: jurij.lah@fkkt.uni-lj.si; gorazd.vesnauer@fkkt.uni-lj.si

Abstract: Knowledge of forces that drive conformational transitions of G-quadruplexes is crucial for understanding the molecular basis of several key cellular processes. It can only be acquired by combining structural, thermodynamic and kinetic information. Existing biophysical and structural evidences on polymorphism of intermolecular G-quadruplexes have shown that the formation of a number of these structures is a kinetically controlled process. Reported kinetic models that have been used to describe the association of single strands into quadruplex structures seem to be inappropriate since the corresponding model-predicted activation energies turn out to be negative. By contrast, we propose here a novel kinetic model that successfully describes experimentally monitored folding/unfolding transitions of G-quadruplexes and gives positive activation energies for all elementary steps, including those describing association of two single strands into bimolecular quadruplex structures. It is based on a combined thermodynamic and kinetic investigation of polymorphic behavior of bimolecular G-quadruplexes formed from d(G₄T₄G₄) and d(G₄T₄G₃) strands in the presence of Na⁺ ions, monitored by spectroscopic (UV, CD) and calorimetric (DSC) techniques. According to our experiment and model analysis the topology of the measured G-quadruplexes is clearly flexible with the conformational forms that respond to the rate of temperature change at which global unfolding/folding transitions occur.

Introduction

The most frequently appearing form of DNA is a double helical structure in which two single strands are held together by Watson–Crick base pairs. In addition, certain DNA sequences that are purine rich and contain tandem repeats of guanines can form more complex, four-stranded structures, called G-quadruplexes.^{1–4} The basic repeating motif in these structures, called G-quartet, comprises four guanine bases held in plane by Hoogsteen hydrogen bonding. The observed high stability of G-quadruplexes is mainly due to this type of hydrogen bonding occurring within each quartet, stacking of hydrophobic quartets upon one another and coordination of monovalent counterions (Na⁺, K⁺) to the eight carbonyl oxygen atoms available to the cation located between the two quartets. The G-quadruplexes may contain one (monomolecular), two (bimolecular) or four (tetramolecular) nucleic acid strands with segments that participate in the formation of the quadruplex structure arranged in a parallel or anti parallel configuration.^{5–7}

It is only recently that the interest in quadruplex DNA has increased, mainly due to the growing evidence that G-quadruplexes may play an important role in some key biological processes. For example, the formation and stabilization of telomeric G-quadruplex structures occurring in the region of the single-stranded overhangs at the ends of chromosomes appear to inhibit the activity of the enzyme telomerase with a consequent senescence or apoptosis of tumor cells.^{8–11} For this reason, stabilization of telomeric G-quadruplexes by selectively bound ligands has emerged as one of the major issues in cancer research.^{12–15} Recently, some quadruplex-forming oligonucleotide aptamers able to bind to certain cellular proteins have been found to inhibit proliferation in various cancer cells.^{16,17} One of these has already been tested in clinical trials as a cancer

- (1) Williamson, J. R. *Annu. Rev. Biophys. Biomol. Struct.* **1994**, *23*, 703–730.
- (2) Keniry, M. A. *Biopolymers* **2000**, *56*, 123–146.
- (3) Neidle, S.; Parkinson, G. N. *Curr. Opin. Struct. Biol.* **2003**, *13*, 275–285.
- (4) Burge, S.; Parkinson, G. N.; Hazel, P.; Todd, A. K.; Neidle, S. *Nucleic Acids Res.* **2006**, *34*, 5402–5415.
- (5) Hardin, C. C.; Perry, A. G.; White, K. *Biopolymers* **2001**, *56*, 147–194.
- (6) Patel, D. J.; Phan, A. T.; Kuryavyi, V. *Nucleic Acids Res.* **2007**, *35*, 7429–7455.
- (7) Dai, J.; Dexheimer, T. S.; Chen, D.; Carver, M.; Ambrus, A.; Jones, R. A.; Yang, D. *J. Am. Chem. Soc.* **2006**, *128*, 1096–1098.
- (8) Blackburn, E. H. *Cell* **1994**, *77*, 621–623.
- (9) Mergny, J.-L.; Hélène, C. *Nature Med.* **1998**, *4*, 1366–1367.
- (10) Parkinson, G. N.; Lee, M. P. H.; Neidle, S. *Nature* **2002**, *417*, 876–880.
- (11) Wheelhouse, R. T.; Sun, D.; Han, H.; Han, F. X.; Hurley, L. H. *J. Am. Chem. Soc.* **1998**, *120*, 3261–3262.
- (12) Read, M.; Harrison, R. J.; Romagnoli, B.; Tanious, F. A.; Gowan, S. H.; Reszka, A. P.; Wilson, W. D.; Kelland, L. R.; Neidle, S. *Proc. Natl. Acad. Sci. U.S.A.* **2001**, *98*, 4844–4849.
- (13) Neidle, S.; Read, M. A. *Biopolymers* **2001**, *56*, 195–208.
- (14) Burger, A. M.; Dai, F.; Schultes, C. M.; Reszka, A. P.; Moore, M. J.; Double, J. A.; Neidle, S. *Cancer Res.* **2005**, *65*, 1489–1496.
- (15) Huppert, J. L. *Biochimie* **2008**, *90*, 1140–1148.
- (16) Bates, P. J.; Kahlon, J. B.; Thomas, S. D.; Trent, J. O.; Miller, D. M. *J. Biol. Chem.* **1999**, *274*, 26369–26377.
- (17) Dapic, V.; Bates, P. J.; Trent, J. O.; Rodger, A.; Thomas, S. D.; Miller, D. M. *Biochemistry* **2002**, *41*, 3676–3685.

therapeutic.¹⁸ In this context it should be emphasized that ligand binding to various DNA sequences depends strongly on the structure of DNA.^{19–27} Therefore, one of the major goals of this research is to explore whether a given G-quadruplex occurs in various structural forms that may exhibit different binding properties.^{28–32} Aside from these studies, the literature contains also few reports on G-quadruplex forming oligonucleotides that act as antiviral agents,^{33,34} as potassium sensing agents³⁵ and as nanowires for molecular electronics.³⁶

There is no doubt that in the recent years a large progress has been made on elucidation of the biological roles of G-quadruplex structures and their polymorphism. Nevertheless, there are still many factors that govern the formation of G-quadruplexes and their physicochemical properties⁵ that are poorly understood. To this purpose X-ray crystallography^{3,4} and NMR spectroscopy^{37,38} can provide important structural information. However, the presence of multiple G-quadruplex species (conformations) in solution and their different kinetics of folding and unfolding may result in contradictory explanations of the observed structural alterations.^{32,38,39} On the other hand, there are several spectroscopic and calorimetric methods that can be used to assign the topology of G-quadruplexes and determine their thermodynamic and kinetic properties. As reported recently, employment of UV spectroscopy in studying thermal stability of G-quadruplexes has shown that some G-quadruplex structures are characterized by hysteresis of their melting and annealing curves. Such typically kinetic behavior observed with UV-melting of bimolecular d(G₄T₄G₄)₂ quadruplex and some of its synthetic analogues has been analyzed in terms of a simple two-

- (18) Teng, Y.; Girvan, A. C.; Casson, L. K., Jr.; Qian, M.; Thomas, S. D.; Bates, P. J. *Cancer Res.* **2007**, *67*, 10491–10500.
- (19) Rentzepis, D.; Marky, L. A. *J. Am. Chem. Soc.* **1992**, *115*, 1645–1650.
- (20) Haq, I.; Ladbury, J. E.; Chowdhry, B. Z.; Jenkins, T. C.; Chaires, J. B. *J. Mol. Biol.* **1997**, *271*, 244–257.
- (21) Chaires, J. B. *Biopolymers* **1997**, *44*, 201–215.
- (22) Lah, J.; Vesnauer, G. *Biochemistry* **2000**, *39*, 9317–9326.
- (23) Lah, J.; Vesnauer, G. *J. Mol. Biol.* **2004**, *342*, 73–89.
- (24) Lah, J.; Carl, N.; Drobak, I.; Šumiga, B.; Vesnauer, G. *Acta Chim. Slov.* **2006**, *53*, 284–291.
- (25) Lah, J.; Drobak, I.; Dolinar, M.; Vesnauer, G. *Nucleic Acids Res.* **2008**, *36*, 897–904.
- (26) Seeniamy, J.; Bashyam, S.; Gokhale, V.; Vankayalapati, H.; Sun, D.; Siddiqui-Jain, A.; Streiner, N.; Shin-ya, K.; White, E.; Wilson, W. D.; Hurley, L. H. *J. Am. Chem. Soc.* **2005**, *127*, 2944–2959.
- (27) Kim, M.-Y.; Vankayalapati, H.; Shin-ya, K.; Wierzbka, K.; Hurley, L. H. *J. Am. Chem. Soc.* **2001**, *124*, 2098–2099.
- (28) Kankia, B. I.; Marky, L. A. *J. Am. Chem. Soc.* **2001**, *123*, 10799–10804.
- (29) Olsen, C. M.; Gmeiner, W. H.; Marky, L. A. *J. Phys. Chem. B* **2006**, *110*, 6962–6969.
- (30) Antonacci, C.; Chaires, J. B.; Sheardy, R. D. *Biochemistry* **2007**, *46*, 4654–4660.
- (31) Kaushik, M.; Suehi, N.; Marky, L. A. *Biophys. Chem.* **2007**, *126*, 154–164.
- (32) Chang, C.-C.; Chien, C.-W.; Lin, Y.-H.; Kang, C.-C.; Chang, T. C. *Nucleic Acids Res.* **2007**, *35*, 2846–2860.
- (33) Rando, R. F.; Ojwang, J.; Elbaggari, A.; Reyes, G. R.; Tinder, R.; McGrath, M. S.; Hogan, M. E. J. *Biol. Chem.* **1995**, *270*, 1754–1760.
- (34) Cherepanov, P.; Esté, J. A.; Rando, R. F.; Reekmans, G.; David, G.; De Clercq, E.; Debyser, Z. *Mol. Pharmacol.* **1997**, *52*, 771–780.
- (35) Ueyama, H.; Takagi, M.; Takenaka, S. *J. Am. Chem. Soc.* **2002**, *124*, 14286–14287.
- (36) Calzolari, A.; Di Felice, R.; Molinari, E.; Garbesi, A. *Appl. Phys. Lett.* **2002**, *80*, 3331–3333.
- (37) Plavec, J.; Cevec, M. *Biochemistry* **2005**, *44*, 15238–15246.
- (38) Luu, K. N.; Phan, A. T.; Kuryavyi, V.; Lacroix, L.; Patel, D. J. *J. Am. Chem. Soc.* **2006**, *128*, 9965–9970.
- (39) Phan, A. T.; Patel, D. J. *J. Am. Chem. Soc.* **2003**, *125*, 15021–15027.

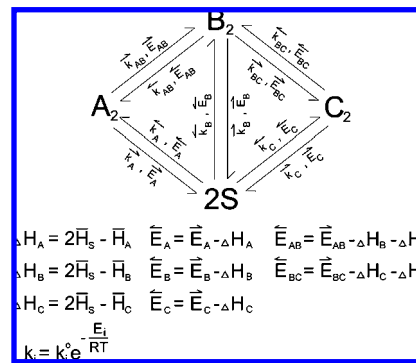


Figure 1. Proposed kinetic model for the thermally induced folding and unfolding of d(G₄T₄G₃)₂ and d(G₄T₄G₄)₂ that assumes coexistence and interconversions of three bimolecular quadruplex structures A₂, B₂ and C₂ and one unfolded single-stranded structure S, characterized by the partial molar enthalpies $\bar{\Delta}H_A$, $\bar{\Delta}H_B$, $\bar{\Delta}H_C$, and $\bar{\Delta}H_S$, respectively. According to Arrhenius each rate constants k_i is expressed in terms of the corresponding frequency factor k_i^0 and activation energy E_i .

state kinetic model.^{37,40–43} The corresponding Arrhenius plots resulted in negative activation energies for the folding transitions, meaning that the formation of the measured bimolecular quadruplexes cannot be considered as an elementary association reaction predicted by the model. Thus, a new explanation has been suggested according to which the melting transition consists of two sequential reactions, an intermolecular premelting reaction followed by the melting transition.³⁷ This suggestion is in qualitative agreement with the recent differential scanning calorimetry (DSC) study of the thermal stability of d(G₄T₄G₄)₂ which has indicated that the measured melting thermograms of samples prepared at moderate cooling rates (0.3–1.0 °C/min) may be deconvoluted into two separate contributions, each reflecting a single melting transition.⁴⁴

In this work we attempt to investigate in detail the polymorphism of d(G₄T₄G₄)₂ and d(G₄T₄G₃)₂ quadruplexes by following their folding and unfolding transitions by UV and CD spectroscopy and DSC. On the basis of the measured DSC thermograms of the two quadruplexes prepared at either very slow (0.05 °C/min) or moderate (1.0 °C/min) cooling rate and unfolded or folded at different moderate heating and cooling rates (0.5–2.0 °C/min) we propose a novel kinetic model of folding/unfolding of G-quadruplexes that suggests coexistence and interconversions of three bimolecular quadruplex structures and one unfolded single-stranded form (Figure 1). We will demonstrate that the proposed model has allowed us, for the first time, to describe the complex nature of G-quadruplex polymorphism monitored at increasing and decreasing temperatures in terms of a single set of kinetic parameters.

Materials and Methods

Sample Preparation. Oligonucleotides d(G₄T₄G₄) and d(G₄T₄G₃) were obtained HPLC pure from Invitrogen Co., Germany, and Midland Co., U.S.A. and used without further purification. Their concentrations in buffer solutions were determined at 25 °C

- (40) Sacca, B.; Lacroix, L.; Mergny, J.-L. *Nucleic Acids Res.* **2005**, *33*, 1182–1192.
- (41) Mergny, J.-L.; Cian, A.; Ghelab, A.; Sacca, B.; Lacroix, L. *Nucleic Acids Res.* **2005**, *33*, 81–94.
- (42) Mergny, J.-L.; Lacroix, L. *Nucleic Acids Res.* **1998**, *26*, 4797–4803.
- (43) Wyatt, J. R.; Davis, P. W.; Freier, S. M. *Biochemistry* **1996**, *35*, 8002–8008.
- (44) Petraccone, L.; Erra, E.; Esposito, V.; Randazzo, A.; Mayol, L.; Nasti, L.; Barone, G.; Giancola, C. *Biochemistry* **2004**, *43*, 4877–4884.

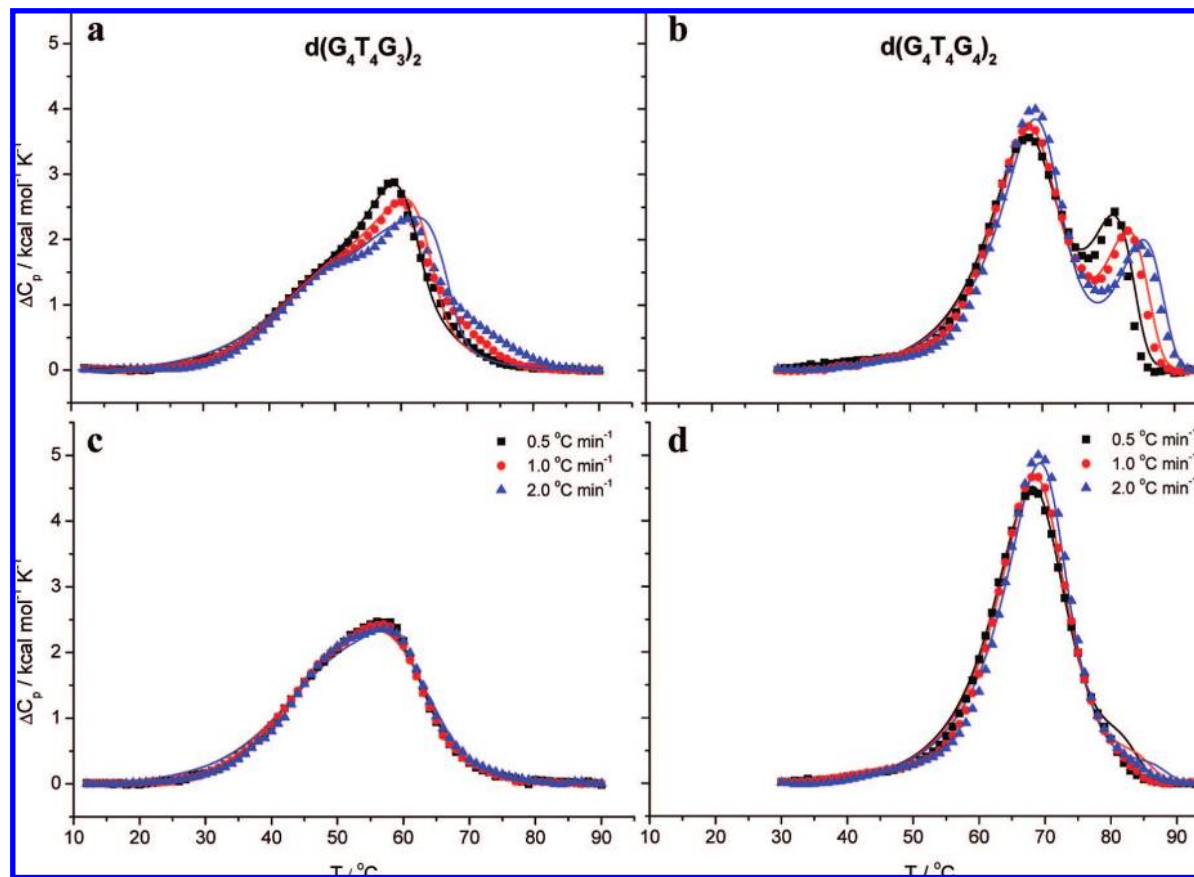


Figure 2. DSC heating ΔC_p versus T curves of $d(G_4T_4G_3)_2$ and $d(G_4T_4G_4)_2$ quadruplexes prepared in the presence of Na^+ ions at either slow ($0.05\text{ }^\circ\text{C}/\text{min}$ -panels a and b) or moderate ($1.0\text{ }^\circ\text{C}/\text{min}$ -panels c and d) cooling rate and recorded at heating rates of 0.5 , 1.0 and $2.0\text{ }^\circ\text{C}/\text{min}$. For clarity reasons only every 11th point is shown. Full lines represent the corresponding ΔC_p values calculated from eqs 4 and 5 using the “best fit” adjustable parameters (Table 1). The concentration of $d(G_4T_4G_3)_2$ and $d(G_4T_4G_4)_2$ was 0.63 mM and 0.51 mM in double strands, $c_{NaCl} = 200\text{ mM}$, $1\text{ cal} = 4.184\text{ J}$.

spectrophotometrically. For the extinction coefficient of their single-stranded forms at $25\text{ }^\circ\text{C}$ we used the values $\varepsilon_{260} = 105,100\text{ M}^{-1}\text{ cm}^{-1}$ for $d(G_4T_4G_3)$ and $\varepsilon_{260} = 115,200\text{ M}^{-1}\text{ cm}^{-1}$ for $d(G_4T_4G_4)$ estimated from the nearest-neighbor data of Cantor et al.⁴⁵ The buffer solutions used in all experiments consisted of 10 mM Na-acetyldiethylamine, 1 mM EDTA and 200 mM NaCl ($pH = 6.9$). The starting solutions of both oligonucleotides were first heated to $100\text{ }^\circ\text{C}$ in an outer thermostat for 5 min to make sure that all DNA is in the unfolded single-stranded form, cooled down to $5\text{ }^\circ\text{C}$ at cooling rates of 0.05 or $1.0\text{ }^\circ\text{C}/\text{min}$ and then used in the DSC or CD experiments. Repeating of heating and cooling cycles (heating at 0.5 , 1.0 or $2.0\text{ }^\circ\text{C}/\text{min}$ followed always by cooling at $1.0\text{ }^\circ\text{C}/\text{min}$) resulted in reproducible calorimetric and spectroscopic melting curves. Characteristically, G-quadruplex samples prepared at the cooling rate of $0.05\text{ }^\circ\text{C}/\text{min}$ show first melting scans being substantially different from the corresponding first melting scans of samples prepared at the cooling rate of $1.0\text{ }^\circ\text{C}/\text{min}$.

UV Melting Experiments. Absorbance versus temperature profiles of DNA samples were measured in a Cary 100 BIO UV/Visible Spectrophotometer (Varian Inc.) equipped with a thermoelectric temperature controller using cells of 0.25 mm path length. Formation of $d(G_4T_4G_4)_2$ and $d(G_4T_4G_3)_2$ quadruplexes ($c \approx 0.5\text{ mM}$ in double strands) at the cooling rate of 0.06 or $1.0\text{ }^\circ\text{C}/\text{min}$ followed by their melting at the heating rate of $1.0\text{ }^\circ\text{C}/\text{min}$ was monitored at $\lambda = 298\text{ nm}$ between 5 and $95\text{ }^\circ\text{C}$. From these data the corresponding UV melting and annealing curves were constructed.

Differential Scanning Calorimetry (DSC). DSC experiments were performed using a Nano DSC II instrument (Calorimetry

Sciences Corp., UT, U.S.A.) and samples prepared in an outer thermostat at the cooling rates of $0.05\text{ }^\circ\text{C}/\text{min}$ and $1.0\text{ }^\circ\text{C}/\text{min}$. Quadruplex concentration used in these DSC studies was about 0.5 mM in double strands. Cyclic DSC measurements were performed at the heating rates of 0.5 , 1.0 and $2.0\text{ }^\circ\text{C}/\text{min}$ and a single cooling rate of $1.0\text{ }^\circ\text{C}/\text{min}$. The measured temperature interval was between 5 and $100\text{ }^\circ\text{C}$. The corresponding baseline (buffer–buffer) scans were subtracted from the unfolding/folding scans prior to their normalization and analysis. The total enthalpy of unfolding or folding, ΔH_{tot} , was obtained from the measured DSC thermograms as the area under the $\Delta C_p = C_p - 2C_{p,S}$ versus T curve, where C_p is the measured heat capacity corrected for the baseline and normalized to 1 mol of quadruplex in double strands and $2C_{p,S}$ is the corresponding heat capacity of the unfolded single-stranded state extrapolated from high temperatures over the whole measured temperature interval (Figure 2).

CD Spectroscopy. CD spectra of the oligonucleotides were measured as a function of temperature in an AVIV CD Spectropolarimeter 62A DS, equipped with a thermoelectric temperature controller. Ellipticity, θ , was measured between 5 and $95\text{ }^\circ\text{C}$ in the temperature intervals of $3\text{ }^\circ\text{C}$ at the average heating rate of $1.0\text{ }^\circ\text{C}/\text{min}$. CD spectra of samples ($\sim 0.5\text{ mM}$ in double strands) prepared at the cooling rate of either 0.05 or $1.0\text{ }^\circ\text{C}/\text{min}$, corrected for the corresponding buffer contribution, were collected between 215 and 320 nm in a 0.25 mm cuvette at $60\text{ nm}/\text{min}$, 2 s signal averaging time and 5 nm bandwidth.

Results and Discussion

Hysteresis of UV Melting Curves. For both, $d(G_4T_4G_4)_2$ and $d(G_4T_4G_3)_2$, that according to the solution NMR and X-ray

(45) Cantor, C. R.; Warshaw, M. M.; Shapiro, H. *Biopolymers* **1970**, *9*, 1059–1077.

crystallographic analysis associate in solution at room temperature into bimolecular quadruplex structures.^{46–49} UV absorbance measurements in the presence of Na^+ ions show hysteresis of UV melting and annealing curves that depends on the heating and cooling rates [Supporting Information, (SI)]. Since both melting curves are completed in the measured temperature interval and the shape of both indicates a biphasic behavior we first tried to explain the observed kinetic characteristics of the measured structural transitions in terms of a simple two-state kinetic model. According to this model the thermally induced unfolding and folding processes were assumed to be elementary reactions of the first and second order, respectively. The observed conformational transitions were discussed using the van't Hoff approach and the rate constants k_{on} and k_{off} were obtained at different temperatures from the corresponding experimentally determined temperature derivatives of the degree of unfolding, $d\alpha/dT$ (SI). Finally, the activation energies of the formation (E_{on}) and dissociation (E_{off}) of the assumed single bimolecular quadruplex structure were determined from the corresponding Arrhenius plots (SI). The negative E_{on} values obtained for both, $d(\text{G}_4\text{T}_4\text{G}_4)_2$ and $d(\text{G}_4\text{T}_4\text{G}_3)_2$, clearly indicate that the formation of neither of the two quadruplexes can be considered as an elementary association reaction. This further means that the suggested two-state model is not appropriate and has to be discarded. At this point it should be mentioned that similar negative E_{on} values have been reported for the formation of some other G-quadruplexes^{50,51} as well as for $d(\text{G}_4\text{T}_4\text{G}_4)_2$.³⁷

Folding and Unfolding of G-Quadruplexes Followed by DSC. Another method that we employed to find out whether the measured melting processes of the two G-quadruplexes involve one or several kinetically governed interconversions and folding/unfolding transitions was DSC. Thermograms of quadruplexes $d(\text{G}_4\text{T}_4\text{G}_4)_2$ and $d(\text{G}_4\text{T}_4\text{G}_3)_2$ measured in the presence of 200 mM NaCl at three different heating rates with the starting sample prepared at very slow or moderate rate of cooling are presented in Figures 2,3. As already mentioned they show a significant dependence on the heating and cooling rate. The most pronounced differences are observed between the DSC heating curves measured at a given heating rate for quadruplex samples prepared by the thermally induced folding at very low (0.05 °C/min) and moderate (1.0 °C/min) cooling rates (Figures 2,3). Those obtained with samples prepared at the slow cooling of 0.05 °C/min clearly show that the measured melting processes involve at least two structural transitions (two peaks). In other words, samples prepared at cooling rate of 0.05 °C/min contain at low temperatures at least two G-quadruplex structures. This is an important difference from the corresponding UV melting curves which appear to occur in a single-step manner (SI). By contrast, samples prepared at the moderate cooling of 1.0 °C/min are characterized by DSC melting curves that reflect for $d(\text{G}_4\text{T}_4\text{G}_3)_2$ at least two structural transitions (broad peak with a weak shoulder) while unfolding of $d(\text{G}_4\text{T}_4\text{G}_4)_2$ seems to occur in a single-step manner (single peak). Furthermore, the DSC cooling curves of $d(\text{G}_4\text{T}_4\text{G}_3)$ and $d(\text{G}_4\text{T}_4\text{G}_4)$ measured at the cooling rate of 1.0 °C/min are also characterized by single peaks

that are close to the mirror images of the corresponding DSC melting curves (Figure 3). Inspection of all our DSC results shows that the total area under the measured DSC thermograms is the same (within few %) regardless of the cooling rate at which the samples were prepared and regardless of the heating rate at which they were unfolded (Figures 2,3). This means that the enthalpies of unfolding of different quadruplex structures in the solution may be considered the same and thus equal to the overall enthalpy of unfolding, ΔH_{tot} , determined from the total area under the measured thermograms as: $\Delta H_{\text{tot}} = (2.91 \pm 0.04) \times 10^5 \text{ J/mol}$ of duplex for $d(\text{G}_4\text{T}_4\text{G}_4)_2$ and $\Delta H_{\text{tot}} = (2.34 \pm 0.04) \times 10^5 \text{ J/mol}$ of duplex for $d(\text{G}_4\text{T}_4\text{G}_3)_2$. It should be emphasized that these ΔH_{tot} values expressed per mole of G-quartets (72.5 kJ/mol for $d(\text{G}_4\text{T}_4\text{G}_4)_2$ and 77.7 kJ/mol for $d(\text{G}_4\text{T}_4\text{G}_3)_2$) agree well with the corresponding literature data^{52–56} (SI). Finally, the DSC melting thermograms of both duplexes prepared at very slow or moderate cooling rates shift with the increasing heating rate to higher temperatures. These shifts can also be considered as an indication of kinetically governed unfolding transitions of the two quadruplexes.

To describe the observed DSC heating and cooling thermograms we tried several kinetic models, all based on the solution NMR and X-ray crystallographic experiments which show that the $d(\text{G}_4\text{T}_4\text{G}_3)$ and $d(\text{G}_4\text{T}_4\text{G}_4)$ conformational space is populated at low temperatures only by bimolecular quadruplex structures.^{46–49} We ended up with the one presented in Figure 1 which allows in the measured temperature interval existence of three kinetically linked quadruplex structures and the corresponding single strands. It is the simplest physically acceptable model that, as shown later, reasonably well describes simultaneously the measured heating and cooling curves in terms of the smallest possible set of adjustable parameters. Simpler model that includes only two dimeric quadruplex species and corresponding single strands turns out to be inappropriate. It leads to a model function that for a given set of adjustable parameters gives a good fit only to heating or cooling curves, but not to both (not shown here). In contrast, more complex models with their more complex model functions result in good fitting to both, heating and cooling curves. Unfortunately, analysis of the corresponding fitting procedures shows that, as a rule, a good fit is obtained mainly due to the increased number of adjustable parameters many of which are highly correlated and thus have no physical meaning.

According to the suggested model (Figure 1), the enthalpy, H , of the measured solution in the DSC sample cell can be expressed as:

$$H = n_2 \bar{H}_2 + n_1 \bar{H}_1 = n_A \bar{H}_A + n_B \bar{H}_B + n_C \bar{H}_C + n_S \bar{H}_S + n_1 \bar{H}_1 \quad (1)$$

where n_1 is the number of moles of solvent, n_2 is the total number of moles of DNA expressed in a double-stranded form, n_A , n_B and n_C are the number of moles of double-stranded quadruplexes A_2 , B_2 and C_2 , n_S is the number of moles of single-stranded unfolded form and \bar{H}_1 , \bar{H}_A , \bar{H}_B , \bar{H}_C and \bar{H}_S are the corresponding partial molar enthalpies. Since $n_S = 2n_2 - 2(n_A + n_B + n_C)$ it follows from eq 1 that:

$$H = n_1 \bar{H}_1 - n_A \Delta H_A - n_B \Delta H_B - n_C \Delta H_C + 2n_2 \bar{H}_S \quad (2)$$

where the quantities $\Delta H_A = 2\bar{H}_S - \bar{H}_A$, $\Delta H_B = 2\bar{H}_S - \bar{H}_B$ and $\Delta H_C = 2\bar{H}_S - \bar{H}_C$ are the enthalpies of unfolding of quadruplex structures A_2 , B_2 and C_2 . By expressing the fractions of quadruplex species present in the solution as $\alpha_A = n_A/n_2$, $\alpha_B = n_B/n_2$ and $\alpha_C = n_C/n_2$ and by taking the temperature derivative

- (46) Haider, S.; Parkinson, G. N.; Stephen, N. *J. Mol. Biol.* **2002**, *320*, 189–200.
- (47) Črnugelj, M.; Hud, N. V.; Plavec, J. *J. Mol. Biol.* **2002**, *320*, 911–924.
- (48) Smith, F. W.; Feigon, J. *Nature* **1992**, *356*, 164–168.
- (49) Schultz, P.; Smith, F. W.; Feigon, J. *Structure* **1994**, *2*, 221–233.
- (50) Bardin, C.; Leroy, J. L. *Nucleic Acids Res.* **1997**, *36*, 477–488.
- (51) Rachwal, P. A.; Findlow, I. S.; Werner, J. M.; Brown, T.; Fox, K. R. *Nucleic Acids Res.* **1997**, *35*, 4214–4222.

Table 1. “Best Fit” Adjustable Parameters Describing the Thermally Induced Folding/Unfolding Transitions of Quadruplexes $d(G_4T_4G_3)_2$ and $d(G_4T_4G_4)_2$ in Terms of the Kinetic Model^a Presented in Figure 1

transition	parameter	$d(G_4T_4G_3)$ value and error ^a	$d(G_4T_4G_4)$ value and error ^a
$A_2 \rightarrow 2S$	\vec{k}_A^0	$(2.1 \pm 0.2) \times 10^{38} \text{ min}^{-1}$	$(5.1 \pm 0.2) \times 10^{45} \text{ min}^{-1}$
$2S \rightarrow A_2$	\vec{k}_A^0	$(4.8 \pm 0.6) \times 10^3 \text{ M}^{-1} \text{ min}^{-1}$	$(2.7 \pm 0.2) \times 10^3 \text{ M}^{-1} \text{ min}^{-1}$
$B_2 \rightarrow 2S$	\vec{k}_B^0	$(9.0 \pm 0.9) \times 10^{40} \text{ min}^{-1}$	$(2.4 \pm 0.2) \times 10^{48} \text{ min}^{-1}$
$2S \rightarrow B_2$	\vec{k}_B^0	$(1.0 \pm 0.1) \times 10^6 \text{ M}^{-1} \text{ min}^{-1}$	$(2.0 \pm 0.1) \times 10^6 \text{ M}^{-1} \text{ min}^{-1}$
$C_2 \rightarrow 2S$	\vec{k}_C^0	$(6.8 \pm 0.2) \times 10^{40} \text{ min}^{-1}$	$(7.5 \pm 0.1) \times 10^{47} \text{ min}^{-1}$
$A_2 \rightarrow B_2$	\vec{k}_{AB}^0	$(6 \pm 2) \times 10^5 \text{ min}^{-1}$	$(4.0 \pm 0.3) \times 10^8 \text{ min}^{-1}$
$B_2 \rightarrow A_2$	\vec{k}_{AB}^0	$(3 \pm 1) \times 10^5 \text{ min}^{-1}$	$(8.0 \pm 0.8) \times 10^8 \text{ min}^{-1}$
$B_2 \rightarrow C_2$	\vec{k}_{BC}^0	$(1.6 \pm 0.2) \times 10^7 \text{ min}^{-1}$	$(7.0 \pm 0.5) \times 10^9 \text{ min}^{-1}$
$C_2 \rightarrow B_2$	\vec{k}_{BC}^0	$(9.00 \pm 0.03) \times 10^6 \text{ min}^{-1}$	$(4.00 \pm 0.04) \times 10^8 \text{ min}^{-1}$
$A_2 \rightarrow 2S$	\vec{E}_A	$(2.43 \pm 0.05) \times 10^5 \text{ J mol}^{-1}$	$(3.00 \pm 0.02) \times 10^5 \text{ J mol}^{-1}$
$B_2 \rightarrow 2S$	\vec{E}_B	$(2.4 \pm 0.4) \times 10^5 \text{ J mol}^{-1}$	$(3.0 \pm 0.3) \times 10^5 \text{ J mol}^{-1}$
$C_2 \rightarrow 2S$	\vec{E}_C	$(2.65 \pm 0.06) \times 10^5 \text{ J mol}^{-1}$	$(3.30 \pm 0.04) \times 10^5 \text{ J mol}^{-1}$
$A_2 \rightarrow B_2$	\vec{E}_{AB}	$(4 \pm 5) \times 10^4 \text{ J mol}^{-1}$	$(6 \pm 1) \times 10^4 \text{ J mol}^{-1}$
$B_2 \rightarrow C_2$	\vec{E}_{BC}	$(6 \pm 3) \times 10^4 \text{ J mol}^{-1}$	$(8 \pm 1) \times 10^4 \text{ J mol}^{-1}$

^a The errors of adjustable parameters were obtained as the square roots of diagonal elements of the corresponding variance-covariance matrix. The experimentally determined $\Delta H_A = \Delta H_B = \Delta H_C = \Delta H_{\text{tot}} = 234 \pm 4 \text{ kJ/mol}$ quadruplex for $d(G_4T_4G_3)_2$ and $291 \pm 4 \text{ kJ/mol}$ quadruplex for $d(G_4T_4G_4)_2$. For both quadruplexes the parameter k_C^0 was set equal to 0 (see text).

of eqs 1 and 2 in combination with the usual assumption that the heat capacity change accompanying the entire unfolding transition of oligo- and polynucleotides is negligibly small one obtains an expression for the partial molar heat capacity of the solute, $\bar{C}_{P,2}$:

$$\bar{C}_{P,2} = \frac{C_p - n_1 \bar{C}_{P,1}}{n_2} = -\frac{d\alpha_A}{dT} \Delta H_A - \frac{d\alpha_B}{dT} \Delta H_B - \frac{d\alpha_C}{dT} \Delta H_C + 2\bar{C}_{P,S} \quad (3)$$

in which C_p is the heat capacity of the measured solution and $\bar{C}_{P,1}$ and $\bar{C}_{P,S}$ are the partial molar heat capacities of solvent and the quadruplex unfolded single-stranded form, respectively. Finally, by extrapolating the measured heat capacity of the unfolded quadruplex form occurring at high temperatures, $2\bar{C}_{P,S}$, over the whole measured temperature interval eq 3 takes the form:

$$\Delta C_p = \bar{C}_{P,2} - 2\bar{C}_{P,S} = -\frac{d\alpha_A}{dT} \Delta H_A - \frac{d\alpha_B}{dT} \Delta H_B - \frac{d\alpha_C}{dT} \Delta H_C \quad (4)$$

The quantity ΔC_p defined in eq 4 can be obtained either experimentally as $\Delta C_p = \bar{C}_{P,2} - 2\bar{C}_{P,S}$ or calculated according to the model presented in Figure 1 as $\Delta C_p = -(d\alpha_A/dT)\Delta H_A - (d\alpha_B/dT)\Delta H_B - (d\alpha_C/dT)\Delta H_C$. As already mentioned, the observed independence of ΔH_{tot} on the heating and cooling rates used in the DSC experiments leads to the conclusion that: $\Delta H_A = \Delta H_B = \Delta H_C = \Delta H_{\text{tot}}$.

The derivation of the $d\alpha/dT$ terms needed to calculate ΔC_p is based on the rates of chemical reactions predicted by the model (Figure 1) combined with the corresponding rate constants and the heating or cooling rates at which the DSC experiments are performed. By expressing these rates as $r = dT/dt$, the total

quadruplex concentration in the single-stranded form as $c_T = c_S + 2c_A + 2c_B + 2c_C$ and the rate constants according to Arrhenius as $k_i = k_i^0 \exp(-E_i/RT)$ (k_i^0 - frequency factor, E_i - activation energy) one obtains:

$$\begin{aligned} -\frac{d\alpha_A}{dT} &= \frac{1}{r} \left[\alpha_A \left(\vec{k}_A^0 \exp\left(-\frac{\vec{E}_A}{RT}\right) + \vec{k}_{AB}^0 \exp\left(-\frac{\vec{E}_{AB}}{RT}\right) \right) - \right. \\ &\quad \left. 2c_T(1 - \alpha_A - \alpha_B - \alpha_C)^2 \vec{k}_A^0 \exp\left(-\frac{\vec{E}_A - \Delta H_A}{RT}\right) - \right. \\ &\quad \left. \alpha_B \vec{k}_{AB}^0 \exp\left(-\frac{(\vec{E}_{AB} - (\Delta H_B - \Delta H_A))}{RT}\right) \right] \\ -\frac{d\alpha_B}{dT} &= \frac{1}{r} \left[\alpha_B \left(\vec{k}_{AB}^0 \exp\left(-\frac{(\vec{E}_{AB} - (\Delta H_B - \Delta H_A))}{RT}\right) + \right. \right. \\ &\quad \left. \left. \vec{k}_B^0 \exp\left(-\frac{\vec{E}_B}{RT}\right) + \vec{k}_{BC}^0 \exp\left(-\frac{\vec{E}_{BC}}{RT}\right) \right) - \alpha_C \vec{k}_{BC}^0 \times \right. \\ &\quad \left. \exp\left(-\frac{(\vec{E}_{BC} - (\Delta H_C - \Delta H_B))}{RT}\right) - \alpha_A \vec{k}_{AB}^0 \exp\left(-\frac{\vec{E}_{AB}}{RT}\right) \right] - \\ &\quad 2c_T(1 - \alpha_A - \alpha_B - \alpha_C)^2 \vec{k}_B^0 \exp\left(-\frac{\vec{E}_B - \Delta H_B}{RT}\right) \\ -\frac{d\alpha_C}{dT} &= \frac{1}{r} \left[\alpha_C \left(\vec{k}_{BC}^0 \exp\left(-\frac{(\vec{E}_{BC} - (\Delta H_C - \Delta H_B))}{RT}\right) + \right. \right. \\ &\quad \left. \left. \vec{k}_C^0 \exp\left(-\frac{\vec{E}_C}{RT}\right) \right) - 2c_T(1 - \alpha_A - \alpha_B - \alpha_C)^2 \vec{k}_C^0 \times \right. \\ &\quad \left. \exp\left(-\frac{(\vec{E}_C - \Delta H_C)}{RT}\right) - \alpha_B \vec{k}_{BC}^0 \exp\left(-\frac{\vec{E}_{BC}}{RT}\right) \right] \end{aligned} \quad (5)$$

Cash–Karp adaptive step-size controlled Runge–Kutta method⁵⁷ was used to solve a set of these differential eqs for a

- (52) Jin, R.; Gaffney, B. L.; Wang, C.; Jones, R. A.; Breslauer, K. J. *Proc. Natl. Acad. Sci. U.S.A.* **1992**, *89*, 8832–8836.
 (53) Mergny, J.-L.; Phan, A.-T.; Lacroix, L. *FEBS Lett.* **1998**, *435*, 74–78.

- (54) Ren, J.; Qu, X.; Trent, J. O.; Chaires, J. B. *Nucleic Acids Res.* **2002**, *30*, 2307–2315.
 (55) Smirnov, I.; Shafer, R. H. *Biochemistry* **2000**, *39*, 1462–1468.

given set of adjustable parameters, and these solutions were used to calculate the model function (eq 4). The “best fit” adjustable parameters were obtained from global fitting the model function to the experimental ΔC_p vs T curves measured at different heating and cooling rates. The fitting procedure was based on the minimization of the corresponding χ^2 function

$$\chi^2 = \sum_i \left(\frac{\Delta C_{p,i}^{\text{eks}} - \Delta C_{p,i}^{\text{mod}}}{\Delta \Delta C_{p,i}^{\text{eks}}} \right)^2 \quad (6)$$

using the SIMPLEX method.⁵⁷ In eq 6 $\Delta C_{p,i}^{\text{eks}}$ and $\Delta C_{p,i}^{\text{mod}}$ are the experimental and model ΔC_p values at a given temperature and $\Delta \Delta C_{p,i}^{\text{eks}}$ is the corresponding experimental error.

According to eqs 4 and 5 the applied model contains a set of adjustable parameters that characterize the kinetics and thermodynamics of all steps in the suggested folding/unfolding mechanism (Figure 1). In Figure 2 is presented the best global fit of the model function (eq 4) to the DSC melting thermograms obtained at different heating rates with samples of both quadruplexes prepared at either slow or moderate cooling rates. Furthermore, in Figure 3 is presented also the best global fit of the model function (eq 4) to the DSC cooling curves that reflect association of d(G₄T₄G₃) and d(G₄T₄G₄) single strands into the corresponding quadruplexes upon cooling from 100 to 5 °C at 1.0 °C/min. These global fits show at different heating and cooling rates a reasonably good agreement with the experiment using for each quadruplex only a single set of adjustable parameters (Table 1). In our opinion this agreement may be considered as a sound support of the model presented in Figure 1. We are well aware that due to the relatively large number of adjustable parameters contained in the model function for ΔC_p the physical meaning of their “best fit” values may be questionable. To address this question we performed the fitting procedure starting with significantly different initial values of the adjustable parameters. The obtained best fit values of all parameters except for \bar{k}_c^0 were always within the error margins presented in Table 1. It appears that the best fit model function is rather insensitive to \bar{k}_c^0 (broad minimum of χ^2 with respect to \bar{k}_c^0). Since the same best global fit was obtained also with setting $\bar{k}_c^0 = 0$, it follows that the predicted 2S → C₂ association is not important for describing the observed thermally induced quadruplex transitions. Despite the introduced simplifications (heat capacity of unfolding for any quadruplex structure is equal to zero, $\Delta H_A = \Delta H_B = \Delta H_C = \Delta H_{\text{tot}}$ and $\bar{k}_c^0 = 0$) the model describes reasonably well the DSC thermograms measured over a wide temperature interval at different heating and cooling rates (a large number of experimental points). However, Figs 2 and 3 show some deviations of the model from the experiment at higher temperatures that may well be due to the simplifications mentioned above. These discrepancies could be reduced by introducing additional adjustable parameters but only at the expense of the physical meaning of the model (high correlation of additional adjustable parameters with the existing ones).

According to the described analysis the fitting procedure provides adjustable parameters that well define only the model predicted 2S ↔ A₂ and 2S ↔ B₂ transitions induced by changing the solution temperature between ~100 and ~5 °C. The

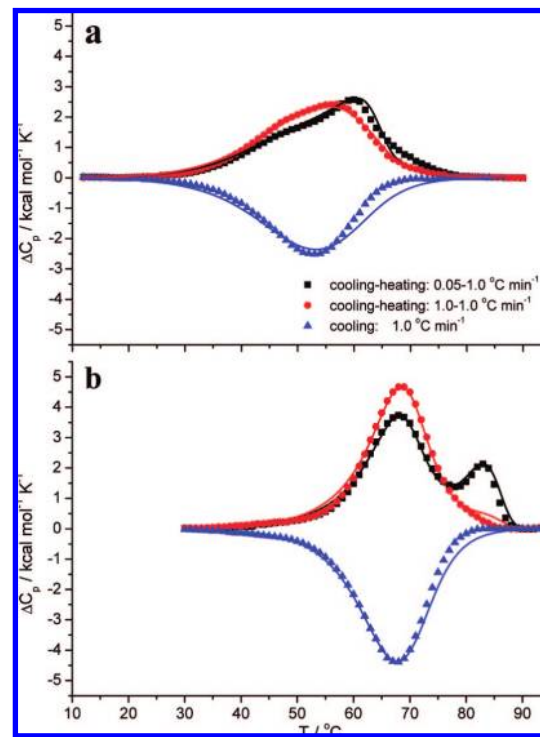


Figure 3. DSC heating ΔC_p versus T curves of d(G₄T₄G₃)₂ (panel a) and d(G₄T₄G₄)₂ (panel b) prepared in the presence of Na⁺ ions by slow (0.05 °C/min) and moderate (1.0 °C/min) cooling rate and heated at a heating rate of 1.0 °C/min in comparison with the corresponding ΔC_p versus T cooling curves measured at the cooling rate of 1.0 °C/min. For clarity reasons only every 11th point is shown. The concentration of d(G₄T₄G₃)₂ and d(G₄T₄G₄)₂ was 0.63 mM and 0.51 mM in double strands, $c_{\text{NaCl}} = 200$ mM. Full lines represent the model-based ΔC_p values calculated from eqs 4 and 5 using the “best fit” adjustable parameters (Table 1); 1 cal = 4.184 J.

corresponding pairs of rate constants \bar{k}_A , \bar{k}_A and \bar{k}_B , \bar{k}_B can be obtained using the Arrhenius relation and the parameters \bar{k}_A^0 , \bar{k}_A^0 , \bar{k}_B^0 , \bar{k}_B^0 , ΔH_A , ΔH_B , \bar{E}_A , and \bar{E}_B (Table 1). They can be further used to express the standard free energy of unfolding of the quadruplex structures A₂ and B₂ as $\Delta G_A^0 = -RT \ln(\bar{k}_A/\bar{k}_A)$ and $\Delta G_B^0 = -RT \ln(\bar{k}_B/\bar{k}_B)$. According to the measured DSC thermograms (Figures 2,3) the heat capacity of unfolding of both quadruplexes may be assumed to be negligible and therefore, the enthalpies of unfolding, ΔH_A and ΔH_B may be considered as temperature-independent quantities. Furthermore, since the DSC measurements were performed at very low concentrations one may assume that $\Delta H_A = \Delta H_A^0$ and $\Delta H_B = \Delta H_B^0$ which means that the corresponding standard entropies of unfolding can be expressed as $\Delta S_A^0 = R \ln(\bar{k}_A^0/\bar{k}_A)$ and $\Delta S_B^0 = R \ln(\bar{k}_B^0/\bar{k}_B)$. Thus, using the “best fit” adjustable parameters from Table 1 and the general relation $\Delta G^0 = \Delta H^0 - T\Delta S^0$ one can express ΔG_A^0 and ΔG_B^0 for d(G₄T₄G₃)₂ in 200 mM NaCl as $\Delta G_A^0 = 234 \text{ kJ mol}^{-1} - 663 \text{ J mol}^{-1} \text{ K}^{-1} \cdot T$ and $\Delta G_B^0 = 234 \text{ kJ mol}^{-1} - 669 \text{ J mol}^{-1} \text{ K}^{-1} \cdot T$. For the d(G₄T₄G₄)₂ quadruplex the corresponding expressions are $\Delta G_A^0 = 291 \text{ kJ mol}^{-1} - 809 \text{ J mol}^{-1} \text{ K}^{-1} \cdot T$ and $\Delta G_B^0 = 291 \text{ kJ mol}^{-1} - 806 \text{ J mol}^{-1} \text{ K}^{-1} \cdot T$. Good agreement between these model-based ΔG_A^0 , ΔG_B^0 , ΔH_A^0 , ΔH_B^0 , ΔS_A^0 and ΔS_B^0 and values expressed per mole of tetrads and those obtained experimentally for several simple “all or none” unfolding transitions of G-quadruplexes^{52–56} may be considered as an additional support of the suggested model (see SI).

Moreover, inspection of Table 1 shows that the best fit of the model function (eq 4) can be obtained with all activation

- (56) Petraccone, L.; Pagano, B.; Esposito, V.; Randazzo, A.; Piccialli, G.; Barone, G.; Mattia, C. A.; Giancola, C. *J. Am. Chem. Soc.* **2005**, *127*, 16215–16223.
 (57) Press, W. H., Flannery, B. P., Teukolsky, S. A. and Vetterling, W. T. *Numerical Recipes in C++*; Cambridge University Press: Oxford, 1992; pp 650–694.

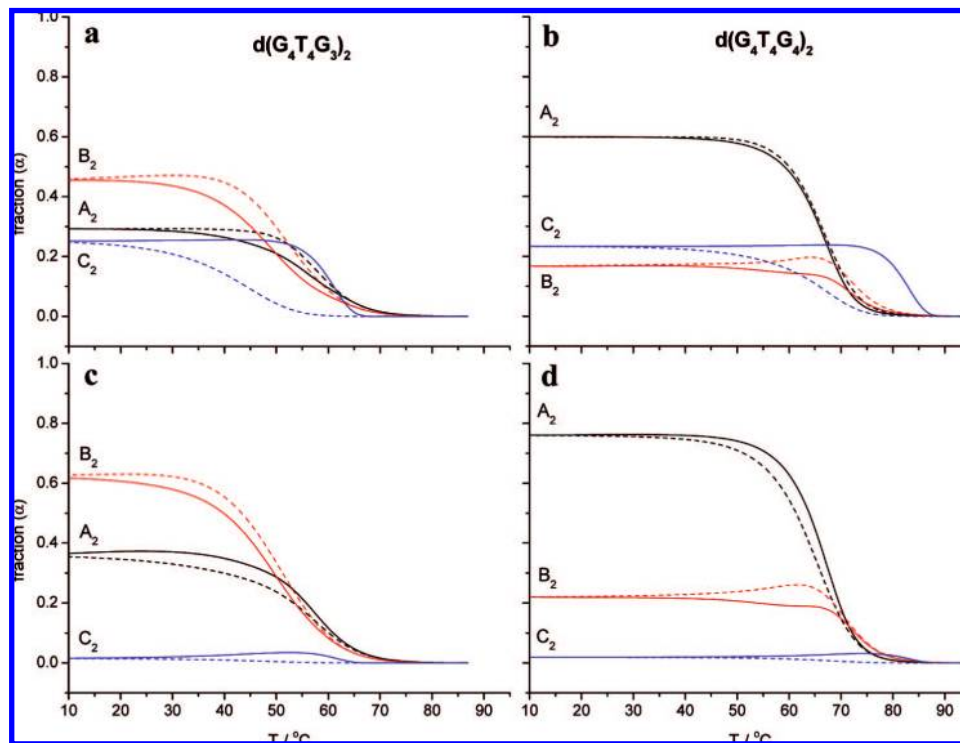


Figure 4. Distribution of species A₂, B₂, C₂ predicted by the model (Figure 1) for the quadruplexes d(G₄T₄G₃)₂ and d(G₄T₄G₄)₂ in 200 mM NaCl solution calculated from eqs 4 and 5 using the “best fit” adjustable parameters (Table 1). Quadruplexes d(G₄T₄G₃)₂ (panel a) and d(G₄T₄G₄)₂ (panel b): formation of structures A₂, B₂, C₂ upon cooling at 0.05 °C/min (dotted lines) and unfolding of these structures upon heating at 1.0 °C/min (full lines). Quadruplexes d(G₄T₄G₃)₂ (panel c) and d(G₄T₄G₄)₂ (panel d): formation of structures A₂, B₂, C₂ upon cooling at 1.0 °C/min (dotted lines) and unfolding of these structures upon heating at 1.0 °C/min (full lines). The concentrations of d(G₄T₄G₃)₂ and d(G₄T₄G₄)₂ were 0.63 mM and 0.51 mM in double strands, respectively.

energies being positive, including those that characterize association of single strands into bimolecular quadruplex structures. This means that all the predicted steps (Figure 1) may be considered as elementary reactions, thus suggesting that the model has a real physical meaning.

The described model analysis provides also the speciation diagrams presented at different heating and cooling rates in Figure 4. Comparison of these α vs T curves calculated for all quadruplex species present in the solution with the corresponding measured DSC thermograms (Figure 2) strongly suggests that the observed high-temperature DSC melting peaks of sample duplexes prepared at a very slow cooling rate reflect the unfolding transitions of the model-predicted quadruplex structure C₂ (Figure 4). It also shows that the observed low-temperature DSC peaks may be considered to result mainly from the combined unfolding transitions of the model-predicted quadruplex structures A₂ and B₂.

G-Quadruplex Topology Followed by CD Spectroscopy. To confirm the observed DSC results and their interpretation based on the proposed model (Figure 1) and to get additional information on the quadruplex structures occurring in the solution we also measured the temperature dependence of CD spectra of d(G₄T₄G₄)₂ and d(G₄T₄G₃)₂ samples prepared at the cooling rates of 0.05 and 1.0 °C/min (Figure 5). It has been shown previously that CD spectroscopy may discriminate between quadruplex topologies having differences in parallel and anti parallel strand orientation. Namely, CD spectra of the model parallel quadruplexes are characterized by a ~264 nm peak and a ~240 nm trough, while those of the model anti parallel quadruplexes exhibit peaks at ~295 nm and troughs at

~265 nm.^{58–61} Thus, one would expect that coexistence and interconversion of G-quadruplex structures containing strands arranged in a parallel and anti parallel orientation can be followed by CD. Strictly speaking, it is the population of syn/anti geometries of guanosine glycosidic torsion angles that seems to determine the shape of CD spectra of G-quadruplexes.⁶⁰ Since this geometry is not directly related to the strand orientation, CD spectroscopy can provide only indicative information on strand orientation.^{62,63} On the other hand, the measured changes of CD peak positions and ratios of their magnitudes do reflect structural (topology) changes of the measured G-quadruplexes. Using this CD-based empirical approach, Miura et al.⁶⁴ have shown that interquadruplex conversion can be controlled by changes in Na⁺ or K⁺ concentrations. They have shown that a phase diagram of the structural conversion between parallel and anti parallel G-quartets of (T₄G₄)₄ depends on the Na⁺ and K⁺ concentrations and on their ratio. According to this diagram both Na⁺ and K⁺ promote at low concentrations anti parallel association ([Na⁺] < 240 mM; [K⁺] < 65 mM) and parallel association at higher concentrations. Similar behavior observed

- (58) Lu, M.; Guo, Q.; Kallenbach, N. R. *Biochemistry* **1993**, *32*, 598–601.
- (59) Balagurumoorthy, P.; Brahmachari, S. K.; Mohanty, D.; Bansal, M.; Sasisekharan, V. *Nucleic Acids Res.* **1992**, *20*, 4061–4067.
- (60) Vortičeková, M.; Chladková, J.; Kejnovská, I.; Fialová, M.; Kypr, J. *Nucleic Acids Res.* **2005**, *33*, 5851–5860.
- (61) Rujan, I. N.; Meleney, J. C.; Bolton, P. H. *Nucleic Acids Res.* **2005**, *33*, 2022–2031.
- (62) Li, J.; Correia, J. J.; Wang, L.; Trent, J. O.; Chaires, J. B. *Nucleic Acids Res.* **2005**, *33*, 4649–4659.
- (63) Bishop, G. R.; Chaires, J. B. In *Current Protocols of Nucleic Acid Chemistry*; Beaucage, S., Ed.; John Wiley & Sons: New York, 2003; Chapter 7, unit 7.11.
- (64) Miura, T.; Benevides, J. M., Jr. *J. Mol. Biol.* **1995**, *248*, 233–238.

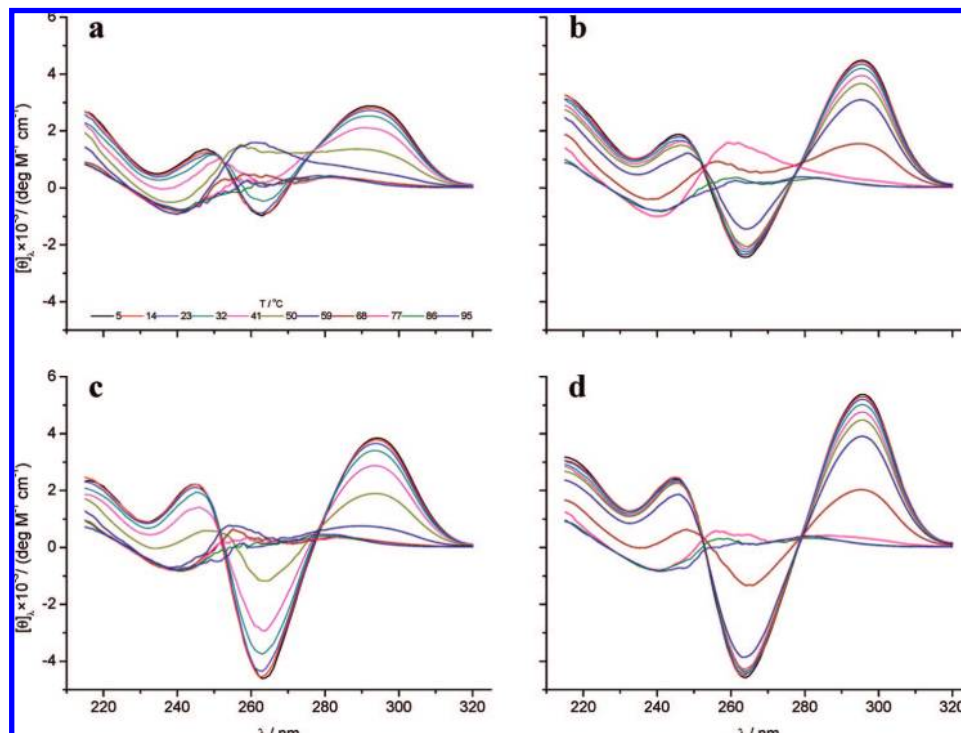


Figure 5. Temperature dependence of CD spectra of quadruplexes $d(G_4T_4G_3)_2$ (panels a, c) and $d(G_4T_4G_4)_2$ (panels b, d) prepared by slow cooling (0.05 $^\circ C/min$ - panels a, b) and moderate cooling (1.0 $^\circ C/min$ - panels c, d). Concentration of duplex $d(G_4T_4G_3)_2$ was 0.63 mM and concentration of duplex $d(G_4T_4G_4)_2$ was 0.51 mM in double strands, $c_{NaCl} = 200$ mM and $l = 0.25$ mm. Temperature was increased in 3.0 $^\circ C$ steps. The measured spectra (ellipticities) were normalized to 1 M double strand concentration and 1 cm path length. For clarity reasons only every third spectrum is shown.

by CD spectroscopy has been reported also for the stabilization of parallel G-quartet structure of $d(G_4T_4G_4)_2$ by divalent cations.^{65–67} In addition, it has been reported recently that the human telomeric repeats $d(TTAGGG)_4$ and $d(TAGGGT-TAGGGT)_2$ can form in the presence of K^+ ions both parallel and anti parallel G-quadruplex structures^{30,39} that can coexist and interconvert in solution and are for $d(TAGGGTTAGGGT)_2$ characterized by a different kinetics of folding and unfolding.³⁹

Our observations are in line with the results of these studies. They show that the temperature dependence of CD spectra of $d(G_4T_4G_4)_2$ and $d(G_4T_4G_3)_2$ quadruplexes formed in the presence of Na^+ ions at the slow cooling rate of 0.05 $^\circ C/min$ differs substantially from the one observed with the samples prepared at the moderate cooling rate of 1.0 $^\circ C/min$ (Figure 5). Such behavior strongly suggests that the association of the $d(G_4T_4G_4)_2$ and $d(G_4T_4G_3)_2$ single strands into the corresponding G-quadruplexes is a kinetically governed process that, depending on the cooling rate, leads to a different composition of G-quadruplex structures formed at low temperatures. Inspection of Figure 5 shows that CD spectra of $d(G_4T_4G_4)_2$ and $d(G_4T_4G_3)_2$ quadruplexes prepared at moderate cooling rates may be ascribed in the entire temperature interval in which the unfolding process occurs only to G-quadruplex structures with CD spectra characteristic of anti parallel strand orientation (we shall denote these structures as AP structures). Namely, at all temperatures between 5 and 95 $^\circ C$ the measured CD spectra show shapes characteristic of the model anti parallel G-quadruplexes. By contrast, samples prepared at the slow cooling rate of 0.05 $^\circ C/$

min show CD spectra and their temperature dependence that may result from a coexistence and interconversion of G-quadruplex structures characterized by CD spectra characteristic of both parallel and anti parallel strand orientation. Thus, around room temperature the observed low intensity at $\lambda = 264$ nm of the measured CD spectra that are characterized by a shape typical of anti parallel G-quadruplex structures may be ascribed to a lower content of the AP structures and a simultaneous compensating contribution of the corresponding content of structures that exhibit CD spectra typical of the parallel strand orientation and will be denoted from now on as PA structures. In the temperature interval between 50 and 70 $^\circ C$ the contribution of these PA structures prevails (switch of CD peak from 295 to 264 nm), indicating that the kinetics of the thermally induced unfolding of AP structures is faster than that of PA structures and/or that with increasing temperature some AP to PA structural conversion takes place. At the highest measured temperatures (~ 95 $^\circ C$) the observed CD signals of both G-quadruplexes are lost, indicating that their PA and AP structures undergo complete unfolding transitions into single-stranded forms.

Comparison of the measured temperature dependence of CD spectra (Figure 5) and the corresponding model-based speciation diagrams (Figure 4) indicates that the PA quadruplex structure corresponds to the model-predicted structure C_2 (Figure 1). Using these speciation diagrams we tried to describe the measured CD melting curves ($\lambda = 264$ nm) of $d(G_4T_4G_4)_2$ and $d(G_4T_4G_3)_2$ by expressing the measured ellipticity, $[\theta]_\lambda$, as a linear combination of A_2 , B_2 , C_2 and S contributions ($[\theta]_\lambda = \sum_i \alpha_i [\theta]_{\lambda,i}; i = A_2, B_2, C_2, S$) and by assuming that the $[\theta]_{\lambda,i}$ values for the AP structures A_2 and B_2 are the same and that molar ellipticities, $[\theta]_{\lambda,i}$, of A_2 , B_2 and C_2 depend linearly on temperature, while the one of single strands remains constant.

(65) Chen, F.-M. *Biochemistry* **1992**, *31*, 3769–3776.

(66) Miyoshi, D.; Nakao, A.; Toda, T.; Sugimoto, N. *FEBS Lett.* **2001**, *496*, 128–133.

(67) Miyoshi, D.; Nakao, A.; Sugimoto, N. *Nucleic Acids Res.* **2003**, *31*, 1156–1163.

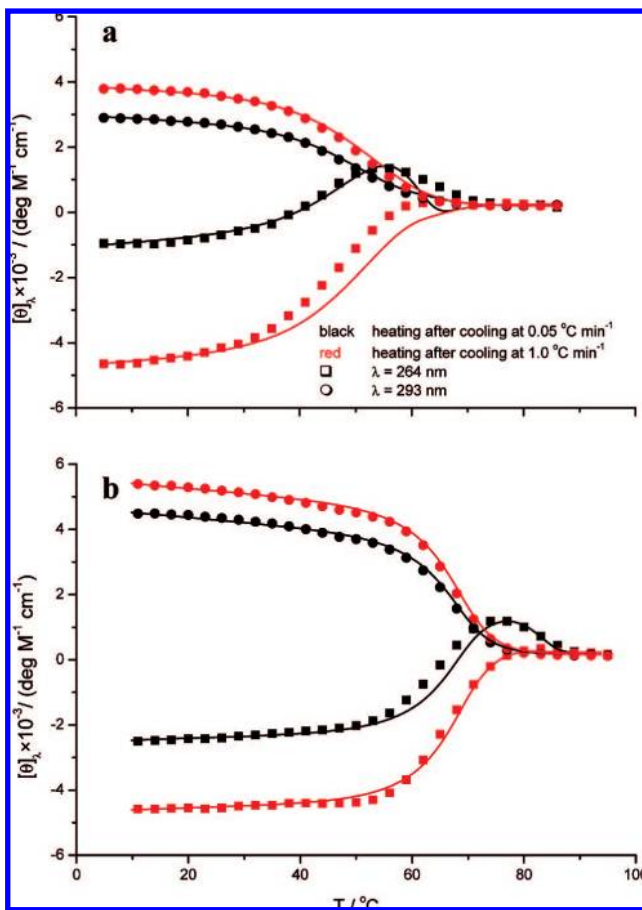


Figure 6. Comparison of the measured (points) and model-based (full line) CD melting curves observed with thermal unfolding (average heating rate of 1.0 °C/min) of quadruplexes $d(G_4T_4G_3)_2$ (panel a) and $d(G_4T_4G_4)_2$ (panel b) prepared at the cooling rate of 0.05 and 1.0 °C/min. The measured ellipticities at $\lambda = 264$ and 293 nm were normalized to 1 M double strand concentration and 1 cm path length. Concentration of duplex $d(G_4T_4G_3)_2$ was 0.63 mM, and concentration of duplex $d(G_4T_4G_4)_2$ was 0.51 mM in double strands, $c_{\text{NaCl}} = 200$ mM.

This assumption is based on the observed linear increase of the measured $[\theta]_{264}$ at low temperatures (Figure 6), where α values for A_2 , B_2 and C_2 are constant (Figure 4). Similarly, since the measured $[\theta]_{264}$ at high temperatures where $\alpha_S = 1$ does not change with temperature, we assumed that $[\theta]_{\lambda,S}$ is temperature independent. The starting $[\theta]_{264,i}$ values were calculated for each quadruplex at the lowest measured temperature from the corresponding $[\theta]_{264}$ values measured for samples prepared at the cooling rate of 0.05 °C/min and 1.0 °C/min and expressed in terms of the corresponding known α values for A_2 , B_2 and C_2 (Figure 4). Using these starting $[\theta]_{264,i}$ values and the constant value of $[\theta]_{264,S}$ together with their assumed linear dependence

on temperature and the known, model-predicted temperature dependence of α for A_2 , B_2 and C_2 (Figure 4) we were able to construct the corresponding model-predicted CD melting curves. Since this reasoning should apply for any λ , we repeated the whole procedure also for $\lambda = 293$ nm. As shown in Figure 6 these model-based CD melting curves appear for both quadruplexes and both wavelengths to be fairly close to those obtained by experiment. We believe that this agreement may be considered as an additional support of the model we propose for the kinetically governed folding/unfolding transitions of $d(G_4T_4G_4)_2$ and $d(G_4T_4G_3)_2$.

Concluding Remarks

In conclusion we would like to emphasize that the observed dependence of the structural composition of G-quadruplex samples on the cooling rate at which they are formed seems to be a general feature of G-quadruplex conformational interconversions. We believe that not paying attention to this phenomenon may be the main reason why, for various G-quadruplexes, a number of different thermodynamic, kinetic and structural data on their thermally induced unfolding/folding transitions have been reported. Furthermore, according to our results, the topology of the measured G-quadruplexes is clearly flexible, with the conformational forms that respond to the rate of temperature changing at which the global unfolding/folding transitions occur. Such responsiveness could allow diverse conformational forms to participate in different biological functions, depending on the conditions at which they occur and on the temperature rate at which these conditions were created. To the best of our knowledge this work represents the first study that underlines the complexity of processes involving G-quadruplexes by discussing kinetics and thermodynamics of their unfolding/folding and interconversion processes in terms of a physically acceptable model mechanism. Nevertheless, comprehensive investigations would be needed to understand in detail transitions of these and other G-quadruplexes in terms of structural features, molecularity, and ion and ligand binding. This, however, remains our future perspective.

Acknowledgment. This work was supported by the Ministry of Higher Education, Science and Technology and by the Agency for Research of Republic of Slovenia through the Grants No. P1-0201 and J1-6653.

Supporting Information Available: (1) UV melting curves described in terms of the two-state kinetic model, (2) statistical analysis, (3) comparison of the results from this study with the literature (Table 2, SI). This material is available free of charge via the Internet at <http://pubs.acs.org>.

JA8026604